Mon. Not. R. Astron. Soc. **300,** L29–L33 (1998)

The birth of a planetary nebula around the carbon star IRC+10216

C. J. Skinner,[1]★† M. Meixner[2] and M. Bobrowsky[3]

[1]*Space Telescope Science Institute, 3700 San Martin Drive, Baltimore, MD 21218, USA*
[2]*Astronomy Department, MC221, 1002 W. Green Street, University of Illinois, Urbana, IL 61801, USA*
[3]*Orbital Sciences Corporation, 7500 Greenway Center Drive, # 700, Greenbelt, MD 20770, USA*

Accepted 1998 August 26. Received 1998 August 26; in original form 1997 November 3

ABSTRACT

Our current understanding of the evolution of solar-type stars suggests that after a period as a red giant star, during which mass loss occurs continuously in the form of a stellar wind, a period of intense mass loss known as a superwind occurs, during which a significant fraction of the envelope of the star is ejected into space, forming the material from which a planetary nebula (PN) will be constructed. It has been suggested that this superwind ejects material from the star in a toroidal or disc-like fashion, rather than isotropically. Here we present *Hubble Space Telescope* optical images of a toroidal superwind caught in the act: our images of the carbon star IRC+10216, which is believed to be in the final stages of red giant evolution, show that most of its optical emission is a bipolar reflection nebula. We show that the full spectral energy distribution and these images can be modelled as an equatorially enhanced dusty superwind, providing the first direct observational support for the toroidal superwind model, and supporting the 'interacting winds' model of PN formation.

Key words: stars: AGB and post-AGB – stars: carbon – circumstellar matter – stars: imaging – stars: individual: IRC+10216 – planetary nebulae: general.

1 INTRODUCTION

Late in their lives, low- and intermediate-mass (0.8–8 solar masses) stars become red giants, which enshroud themselves in dusty cocoons by their massive stellar winds. Eventually the hot interior regions of the star become exposed, ionizing the expelled red giant wind and producing a planetary nebula (PN). While most red giant winds are roughly spherical, most PNe are elliptical or bipolar (e.g. Zuckerman & Aller 1986; Olofsson 1993). It has been proposed that this axial symmetry results from the interaction of a fast stellar wind from the hot central star with a dense, equatorially concentrated envelope, generated in the red giant mass-loss phase (Kwok, Purton & Fitzgerald 1978). The fast wind is funnelled along the polar axes, evacuating a biconical region and generating a bipolar nebula. It has been suggested (e.g. Iben & Renzini 1983; Skinner et al. 1995) that at the end of red giant evolution there is a 'superwind' phase, when the stellar wind becomes very intense and toroidal.

IRC+10216 is amongst the most important sources in the study of red giant evolution. Soon after its discovery in the IRC all-sky infrared (IR) survey (Neugebauer & Leighton 1969), it was recognized to be optically highly obscured but the second-brightest non-solar system IR source in the sky (Becklin et al. 1969). Further study soon showed it to be a C star (a red giant with its atmosphere heavily carbon-enriched by dredge-up of nuclear-processed material from the interior) surrounded by a massive, dust-laden molecular envelope (Miller 1970; Herbig & Zappala 1970). Observations of the mm-wavelength rotational spectral lines of various molecules (e.g. Bieging & Rieu 1989; Groesbeck, Phillips & Blake 1994; Dayal & Bieging 1995) show that at large radii (greater than 10^{16} cm, or about 200 stellar radii) the envelope is expanding in a more or less spherically symmetric fashion at a velocity of about 14.5 km s^{-1}, typical of red giant winds. Detailed modelling of the radiative transfer of these spectral lines through the expanding envelope shows that the mass-loss rate is of order $2–5 \times 10^{-5}$ $M_\odot$ yr^{-1} ($1\ M_\odot = 1$ solar mass). Through a similarly detailed treatment of the radiative transfer of the full stellar spectral energy distribution through the dusty envelope, including the effects of absorption by dust grains, which are heated and re-emit the radiation at longer wavelengths, and scattering by grains, a dust mass-loss rate can be obtained (e.g. Rowan-Robinson et al. 1986; Bagnulo, Doyle & Griffin 1995).

Both these techniques have almost always assumed spherical symmetry in the radiative transfer solution. Observations show this to be true in the case of IRC+10216 far from the star (e.g. Bieging & Rieu 1989; Dayal & Bieging 1995), but close to the star it has appeared that the envelope might follow axial, rather than spherical, symmetry (e.g. Becklin et al. 1969; Kastner & Weintraub 1994). Thus IRC+10216 would appear to be a promising source to investigate, with respect to the complicated transition between red giants and PNe.

★ On assignment from the Space Sciences Division of the European Space Agency.
† Deceased 1997 October.

2 OBSERVATIONS

We have obtained images of this intriguing source using the Wide Field and Planetary Camera 2 (WFPC2; Biretta et al. 1996) aboard the *Hubble Space Telescope* (*HST*). The images were taken as part of an *HST* snapshot survey of evolved stars, using a broad-band filter with a mean wavelength of 0.8269 μm (hereafter F814W), and comprising a pair of exposures of duration 300 s. The images were processed by the STScI WFPC2 calibration pipeline software, and subsequently combined with cosmic ray rejection following the techniques developed for the *Hubble Deep Field* image processing (Williams et al. 1996). The resulting F814W image is shown in Fig. 1, and shows a compact bipolar reflection nebula. The brighter point-like source in the southern lobe of the reflection nebula is probably the central star of IRC+10216; just barely seen in our WFPC2 image and comprising just a few per cent of the apparent luminosity at this wavelength.

In Fig. 2 we show a WFPC2 image of the Cygnus Egg Nebula, CRL2688. CRL2688 is often regarded as the prototypical proto-planetary nebula, an object in transition between the red giant and PN phases (Sahai et al. 1998). It is also a bipolar reflection nebula, in which the central star is completely hidden behind a dense, dusty, equatorial torus or disc, which is seen as a dark band across the centre of the nebula. The central star of CRL2688 can be classified by its spectrum, seen in reflection in the nebula, although the star is not seen directly at any wavelength. There are strong morphological similarities between CRL2688 and IRC+10216: both have a pair of bipolar lobes; a set of faint outer concentric rings or arcs are seen around CRL2688, which may correspond to discrete phases of heavy mass loss, and there are hints of similar structure around IRC+10216; a pair of horns pointing north out of IRC+10216 resembles pairs of horns pointing out of both bipolar lobes of CRL2688; both have a dark band across the 'waist' of the nebula.

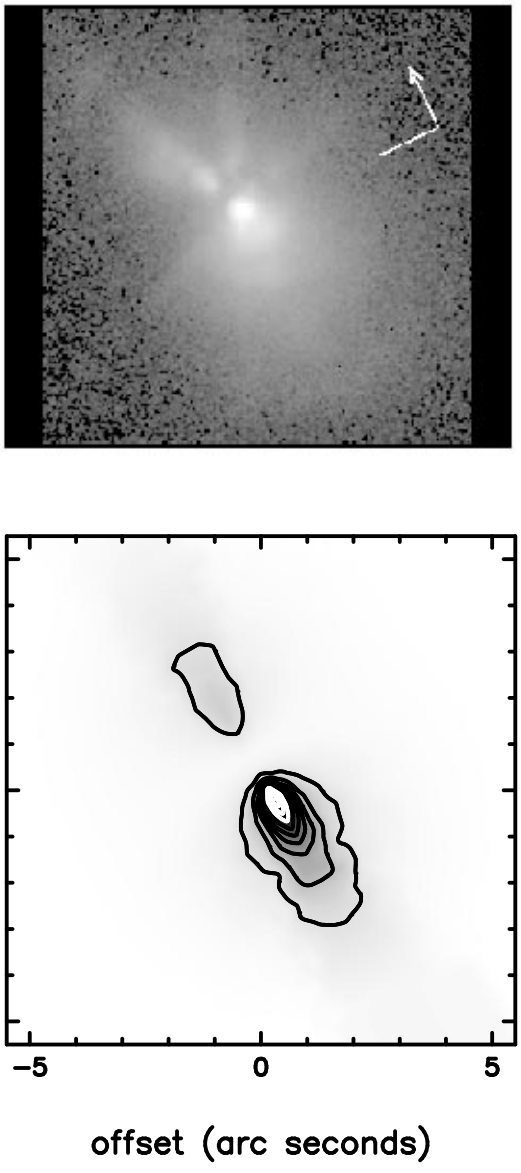

Figure 1. Upper panel: *HST* WFPC2 image of IRC+10216 using the F814W filter. The pixel scale is 0.046 arcsec, corresponding to 1.4×10^{14} cm at its estimated distance of 170 pc. The total field of view displayed here is 11.8 arcsec. The grey-scale is set to a minimum (black) surface brightness of 1.7×10^{-7} Jy arcsec^{-2} and a maximum (white) surface brightness of 5.4×10^{-3} Jy arcsec^{-2}. (1 Jansky $= 10^{-26}$ Wm^{-2} Hz^{-1}). A compass shows the directions of north (with an arrow) and east (no arrow) on the sky. Lower panel: simulated 0.8-μm image of the reflection nebulosity of IRC+10216 from our radiative transfer model (see text and Table 1). The direct light from the central star is not included in this simulated image. Contour spacing is logarithmic, with the lowest contour at 1 per cent of the peak surface brightness. Grey-scale goes from white (minimum) to black (maximum). Axes are labelled in arcsec on the sky. The field of the view of this image is identical to that shown in the upper panel.

3 RADIATIVE TRANSFER MODEL

We have previously generated models of CRL2688 using an axially symmetric full radiative transfer code, which models the transport of radiation (by scattering, absorption and re-emission by dust grains) through a dusty disc or torus (Collison & Fix 1991; Skinner et al. 1997). With such a model we obtained reasonable fits to the complete IR to mm-wavelength spectral energy distribution of

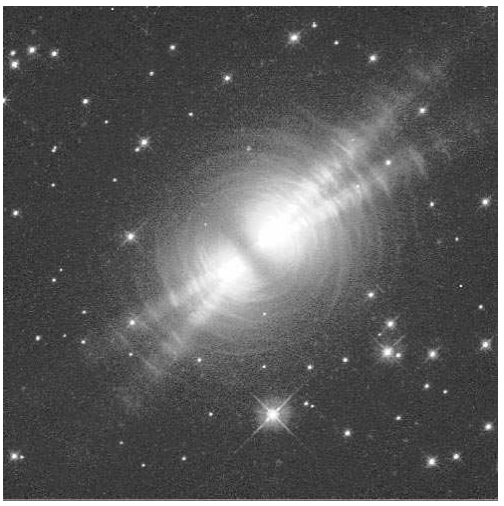

Figure 2. *HST* WFPC2 image of the Cygnus Egg Nebula, CRL2688, via the F606W filter, for the purposes of comparison with IRC+10216. (This image was created with support from the Space Telescope Science Institute, operated by the Association of Universities for Research in Astronomy, Inc., under NASA contract NASS-26555, and is reproduced with permission from AURA/STScI.) The pixel scale is 0.2 arcsec, corresponding to 5.4×10^{15} cm at a distance of 1.8 kpc. The total field of view displayed is approximately 80 arcsec. The image has been discussed by Sahai et al. (1998).

Table 1. IRC+10216 model parameters.

Parameter	Value	Source
Stellar effective temperature	2010 K	WDS
Stellar radius	8.0×10^{13} cm	model
Distance	170 pc	KW,WDS
Luminosity	2.0×10^4 $L_\odot$	model
Dust shell inner radius	$4.0R_*$	model
Outflow velocity	14.5 km s^{-1}	GPB
Dust mass-loss rate	1.0×10^{-7} $M_\odot$ yr^{-1}	model
amorphous carbon : SiC : $Mg_{0.9}Fe_{0.1}S$ by mass	92 : 3 : 5	model
Minimum grain radius, r_{min}	0.04 μm	model
Maximum grain radius, r_{max}	0.4 μm	model
Grain size distribution index, α	−1	model
Bipolar axis inclination to sky	$20 \pm 10°$	model
Equator/pole density ratio	10	model
Bicone opening angle	15°	model

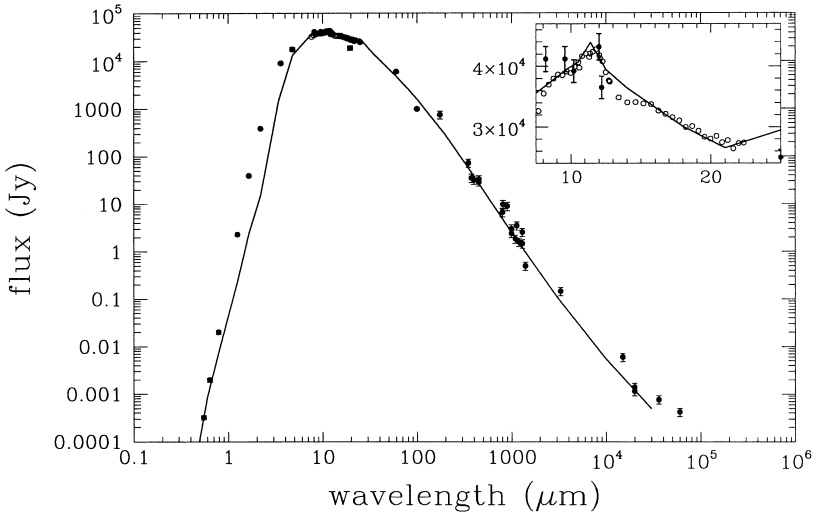

Figure 3. Spectral energy distribution of our axially symmetric radiative transfer model of IRC+10216 (solid line) compared with previously published observations (sources can be found in Bagnulo et al. 1995). The inset shows the 8–24 μm spectrum from the *InfraRed Astronomical Satellite*, *IRAS*, (plotted as open circles) as well as ground-based photometry (filled circles with error bars) compared with the model (solid line): the upturn of the model at the long-wavelength end is due to the 30-μm MgS dust emission feature.

CRL2688, and good simulations of optical and IR images of the nebula. To investigate the apparent similarity between these two objects, we have modelled IRC+10216 using the same radiative transfer code. The parameters used in the model are summarized in Table 1. The model dust shell is toroidal in the inner region with an equator to pole density ratio of 10, becoming spherical beyond a radius of about 100 photospheric radii. The total mass-loss rate was constant in the model, implying that the mass-loss rate has recently increased in the equatorial direction but decreased in the polar direction. The equations used to characterize the density distribution are given by Skinner et al. (1997). The density was fixed in a biconical region extending 15° either side of the polar axes, yielding a final density distribution remarkably similar to that deduced for CRL2688 by Skinner et al. (1997). A distribution of dust grain sizes and types was simulated by synthesizing a mean grain, the size, grain absorption and scattering properties of which as functions of wavelength represent averages over a distribution of grain sizes, calculated using Mie theory (e.g. Rowan-Robinson & Efstathiou 1993). The synthesized grains used the size distribution properties listed in Table 1, and the grain types employed were amorphous carbon (Rouleau & Martin 1991), SiC (Pégourié 1988) and $Mg_{0.9}Fe_{0.1}S$ (Begemann et al. 1994), which appear from both observations and theory to be the dominant condensates in red giant winds. A grain size distribution was used where the number of grains of radius r is proportional to r^α (α is a constant), with minimum and maximum radii r_{min} and r_{max}. The dust mass-loss rate of 1.0×10^{-7} $M_\odot$ yr^{-1} would lead, with a canonical C star gas-to-dust ratio of order 200, to a total gas mass-loss rate of about 2×10^{-5} $M_\odot$ yr^{-1}, consistent with measurements from mm-wavelength molecular lines (e.g. Bieging & Rieu 1989; Dayal & Bieging 1995; Truong-Bach, Morris & Rieu 1991).

Fig. 3 shows our model spectral energy distribution for IRC+10216, and Fig. 1 shows the model image for a wavelength of 0.8 μm. Both the spectral energy distribution and the image were calculated using an inclination angle of the bipolar axis of 20° to the plane of the sky. At inclination angles smaller than 10° the reflection lobes become similar in surface brightness, while at larger inclination angles than 30° the fainter reflection lobe disappears (it becomes heavily extinguished by the equatorial region, which obscures more and more of the fainter lobe as the inclination angle increases). The results indicate that the circumstellar envelope has to be strongly toroidal close to the star. The sudden change

in density, by a few tens of per cent, at the edge of the bicone, is consistent with the presence of a faster bipolar outflow punching its way through the envelope. There are hints in profiles of mm-wavelength spectral lines that such a faster outflow may be present (Truong-Bach et al. 1991), but the evidence is inconclusive. The model fits the data well in the optical and at all wavelengths from 7.5 μm longwards, but the fit is not so good in the 1.6–4.8 μm region. The *IRAS* 8–22 μm spectrum has been used as a major constraint on our model, but the ground-based photometry in this region, which was obtained at the same epoch as all the near-IR and visible photometry plotted in Fig. 3, shows a different spectral slope to the *IRAS* spectrum, which was obtained at a somewhat different epoch. Thus, because the star is strongly (but fairly predictably) variable, caution must be exercised in interpreting a full spectral energy distribution. To better constrain the model, we need resolved images in the near-IR, which will strongly constrain the grain size distribution and stellar effective temperature (the star becomes directly visible in the near-IR, and the reflection nebula shrinks in angular extent with increasing wavelength, in a manner dependent on grain size distribution). With these constraints, we should be able to generate a unique model providing strong constraints for an evolutionary scenario. The current model is primarily an illustration that the general properties of the IRC+10216 nebula are reproducible with a toroidal superwind model.

4 DISCUSSION

Since the molecular rotational lines show that a few arcsec from the star the envelope is more or less spherical (Dayal & Bieging 1995), we can now state that the mass-loss process for IRC+10216 has evolved from one that is basically isotropic to one that is strongly equatorially enhanced during the past 200 yr. However, the total mass-loss rate, based on our dust model and on previous molecular line models (e.g. Bieging & Rieu 1989; Truong-Bach et al. 1991; Olofsson 1993; Dayal & Bieging 1995), does not appear to have changed significantly over the same period. Our models of various post-AGB stars imply that some stars (e.g. CRL2688) undergo a dramatic increase in mass-loss rate during a toroidal superwind phase (Skinner et al. 1997), whereas others may undergo a smaller increase during this phase (Meixner et al. 1997). IRC+10216 may be one of the latter group. These observations and our model imply that the change in mass-loss behaviour from isotropic to equatorially enhanced is not inevitably accompanied by a large and simultaneous increase in mass-loss rate. Instead, based on this scenario, the morphological change of behaviour appears to be a regular part of red giant evolution, and the enormous mass-loss rate increases reported for some stars may be an unrelated phenomenon, or one that follows the onset of toroidal mass loss. Some superwind models suggest that equatorially enhanced mass loss might result from engulfment of a binary companion star by the expanding red giant, with transfer of angular momentum into the red giant wind (Morris 1987). The apparent rapid change from isotropic to equatorially enhanced mass loss in IRC+10216, with no significant change in mass-loss rate, does not at first sight appear consistent with such a model. For the same reasons our observations argue against the influence of a remnant protostellar dust disc, the inertia of which has been suggested as a means to focus a spherical outflow into a bipolar one (e.g. Balick & Preston 1987). A change in the structure of the red giant envelope appears more likely to be responsible.

These observations represent a fundamental advance in our understanding of post-AGB evolution. Examples of non-spherical mass loss from red giants are few in number but well known. The prime examples are OH231.8+4.2 and the C star V Hya. Both of these sources show evidence for a rather unusual nature. OH231.8+4.2 has very long, highly collimated jets with high velocity (Cohen et al. 1985; Reipurth 1987), and has Herbig–Haro (HH) objects entrained in them. It is also believed to have a hot stellar companion (Cohen et al. 1985), making it somewhat resemble a symbiotic star system. The bipolar flow is at least 1300 years old (Reipurth 1987), indicating that very fast jets have been established while the evolved star is still a red giant, a situation which is not readily explainable in terms of the interacting wind model for bipolar PN generation. V Hya is very similar, having a fast bipolar flow seen in molecular lines (Tsuji et al. 1988; Kahane et al. 1996) and in optical emission lines (Lloyd Evans 1991). V Hya has been found to be a rapid rotator, and is therefore thought to be a common envelope binary (Barnbaum, Morris & Kahane 1995). These are the only two red giants known to possess fast bipolar outflows, and they also bear the distinction of being close binaries. IRC+10216, in contrast, is clearly not a rapid rotator, has no evidence for any companion, and, if it has a bipolar component to its outflow, its velocity does not exceed by much the general, isotropic outflow usually observed in molecular lines. However, there is observational evidence, supported by modelling, for IRC+10216 having evolved from a spherical to a toroidal outflow source in the past few hundred years, something never before observed in a solitary red giant. We suggest a scenario whereby IRC+10216 is in the process of evolving off the AGB into its PN phase, with the onset of a toroidal mass-loss phase that will ultimately lead, via the interacting wind process (Kwok et al. 1978), to a bipolar PN.

Our snapshot survey of evolved stars using WFPC2 is still in progress. To date IRC+10216 is the only extreme red giant star that has been observed in the survey. We hope that further stars at this fascinating evolutionary stage will be observed, to shed further light on the remarkable dynamic processes at work in these stars. Being a snapshot survey, the exposures we obtain are not very long. Exposures of much longer duration of this and similar sources will hopefully be obtained in the future, to reveal structure in the nebulae further from the stars, which may reveal details of their past mass-loss history. We also hope to obtain near-IR *HST* images with which to improve our model.

ACKNOWLEDGMENTS

These observations were obtained at the Space Telescope Science Institute, which is operated by the Association of Universities for Research in Astronomy, Inc., under NASA contract NAS 5-26555. MB was supported by NASA STScI Grant GO-06364.01-95A. MM was supported by NASA STScI Grant GO-06364.02-95A. Chris Skinner passed away on 1997 October 20, and will be remembered as an excellent astronomer and good friend.

REFERENCES

Bagnulo S., Doyle J. G., Griffin I. P., 1995, A&A, 301, 501
Balick B., Preston H. L., 1987, AJ, 94, 958
Barnbaum C., Morris M., Kahane C., 1995, ApJ, 450, 862
Becklin E. E., Frogel J. A., Hyland A. R., Kristian J., Neugebauer G., 1969, ApJ, 158, L133
Begemann B., Dorschner J., Henning T., Mutschke H., Thamm E., 1994, ApJ, 423, L71
Bieging J. H., Rieu N.-Q., 1989, ApJ, 329, L107

Biretta J. A. et al., 1996, WFPC2 Instrument Handbook, Version 4.0. STScI, Baltimore
Cohen M., Dopita M. A., Schwartz R. D., Tielens A. G. G. M., 1985, ApJ, 297, 702
Collison A. J., Fix J. D., 1991, ApJ, 368, 545
Dayal A., Bieging J. H., 1995, ApJ, 439, 996
Groesbeck T. D., Phillips T. G., Blake G. A., 1994, ApJS, 94, 147 (GPB)
Herbig G. H., Zappala R. R., 1970, ApJ, 162, L15
Iben I., Renzini A., 1983, ARA&A, 21, 271
Kahane C., Audinos P., Barnbaum C., Morris M., 1996, A&A, 314, 871
Kastner J. H., Weintraub D. A., 1994, ApJ, 434, 719 (KW)
Kwok S., Purton C. R., Fitzgerald P. M., 1978, ApJ, 219, L125
Lloyd Evans T., 1991, MNRAS, 248, 479
Meixner M., Skinner C. J., Graham J. R., Keto E., Jernigan J. G., Arens J. F., 1997, ApJ, 482, 897
Miller J. S., 1970, ApJ, 161, L95
Morris M., 1987, PASP, 99, 1115
Neugebauer G., Leighton R. B., 1969, Two micron sky survey: a preliminary catalog. NASA SP, Washington, DC
Olofsson H., 1993, in Schwartz H. E., ed., Proc. 2nd ESO/CTIO Workshop, Mass Loss on the AGB and Beyond. ESO, Garching-bei-München, p. 330
Pégourié B., 1988, A&A, 194, 335
Reipurth B., 1987, Nat, 325, 787
Rouleau F., Martin P. G., 1991, ApJ, 377, 526
Rowan-Robinson M., Efstathiou A., 1993, MNRAS, 263, 675
Rowan-Robinson M., Lock T. D., Walker D. W., Harris S., 1986, MNRAS, 222, 273
Sahai R. et al., 1998, ApJ, 493, 301
Skinner C. J., Meixner M., Barlow M. J., Justtanont K., Arens J. F., Jernigan J. G., 1995, in Watt G. D., Williams P. M., eds, Circumstellar Matter 1994. Kluwer, Dordrecht, p. 383
Skinner C. J. et al., 1997, A&A, 328, 290
Truong-Bach, Morris D., Nguyen-Q-Rieu, 1991, A&A, 249, 435
Tsuji T., Unno W., Kaifu W., Izumiura H., Ukita N., Cho S., Koyama K., 1988, ApJ, 327, L23
Williams R. E. et al., 1996, AJ, 112, 1335
Zuckerman B., Aller L. H., 1986, ApJ, 301, 772

This paper has been typeset from a TEX/LATEX file prepared by the author.